(469219) Kamoʻoalewa, A Space Weathering Matured Small NEA: Target of the Tianwen-2 Sample-Return Mission

Pengfei Zhang[1], Guozheng Zhang[2], Xiaoran Yan[3], Mikael Granvik[4,5], Yongxiong Zhang[6], Yunbo Niu[7], Ronghua Pang[1], Zichen Wei[8], Pengyue Wang[2], Qinwei Zhang[9], Xuejin Lu[10], Shoucun Hu[9], Bin Cheng[3], Pierre Vernazza[11], Takahiro Hiroi[12], Edward Cloutis[13], Francesca DeMeo[14], Te Jiang[8], Pierre Beck[15], Wing-Huen Ip[16], Marco Fenucci[17,18], Haibin Zhao[9], Xiaobin Wang[19], Xiaoping Lu[2], Jiang Zhang[10], Zongcheng Ling[10], Cateline Lantz[20], Jooyeon Geem[21], Xing Wu[22], Honglei Lin[23], Sizhe Zhao[2], Juntao Wang[24], Zhiping He[25], Yonglong Zhang[26], Liyong Zhou[27], Xiliang Zhang[19], Shijei Li[1], Sen Hu[23], Wei Yang[23], Xiongyao Li[1], Xiaoping Zhang[2], Jiahui Liu[2], Peng Zhang[28], Guang Zhang[28], Yangting Lin[23] & Yang Li[1]✉

[1]Center for Lunar and Planetary Sciences, Institute of Geochemistry, Chinese Academy of Sciences, Guiyang, China.

[2]State Key Laboratory of Lunar and Planetary Sciences, Macau University of Science and Technology, Macau, China.

[3]School of Aerospace Engineering, Tsinghua University, Beijing, China.

[4]Department of Physics, University of Helsinki, Helsinki, Finland.

[5]Asteroid Engineering Laboratory, Luleå University of Technology, Kiruna, Sweden

[6]School of Engineering, Guangzhou College of Technology and Business, Guangzhou, China.

[7]Institute of Systems Engineering, Macau University of Science and Technology, Macau, China.

[8]School of Earth Sciences, China University of Geosciences, Wuhan, China.

[9]Key Laboratory of Planetary Sciences, Purple Mountain Observatory, Chinese Academy of Sciences, Nanjing, China.

[10]Shandong Key Laboratory of Optical Astronomy and Solar-Terrestrial Environment, School of Space

Science and Physics, Institute of Space Sciences, Shandong University, Weihai, China.
[11]Aix Marseille Université, CNRS, CNES, Laboratoire d'Astrophysique de Marseille, Marseille, France.
[12]Department of Geological Sciences, Brown University, Providence, USA.
[13]Department of Geography, University of Winnipeg, Winnipeg, Canada.
[14]Department of Earth, Atmospheric, and Planetary Sciences, Massachusetts Institute of Technology, Cambridge, USA.
[15]UJF-Grenoble 1/CNRS-INSU, Institut de Planétologie et d'Astrophysique de Grenoble, Grenoble, France.
[16]Institute of Astronomy, National Central University, Chung Li, Taiwan, China.
[17]ESA ESRIN/PDO/NEO Coordination Centre, Largo Galileo Galilei, Frascati (RM), Italy.
[18]Elecnor Deimos, Via Giuseppe Verdi, San Pietro Mosezzo (NO), Italy.
[19]Yunnan Observatories, Chinese Academy of Sciences, Kunming, China.
[20]Institut d'Astrophysique Spatiale, CNRS/Université Paris Saclay, Paris, France.
[21]Department of Physics and Astronomy, Seoul National University, Seoul, Republic of Korea.
[22]State Key Laboratory of Space Weather, National Space Science Center, Chinese Academy of Sciences, Beijing, China.
[23]Key Laboratory of the Earth and Planetary Physics, Institute of Geology and Geophysics, Chinese Academy of Sciences, Beijing, China.
[24]Institute of Deep Space Sciences, Deep Space Exploration Laboratory, Hefei, China.
[25]Shanghai Institute of Technical Physics, Chinese Academy of Sciences, Shanghai, China.
[26]The College of Mechanical and Vehicle Engineering, Taiyuan University of Technology, Taiyuan, China.
[27]School of Astronomy and Space Science & MOE Key Laboratory of Modern Astronomy and Astrophysics, Nanjing University, Nanjing, China.
[28]Technology and Engineering Center for Space Utilization, Chinese Academy of Sciences, Beijing, China.

Corresponding Author: Yang Li (liyang@mail.gyig.ac.cn)

Supplementary

Figures 1–7

Tables 1–2

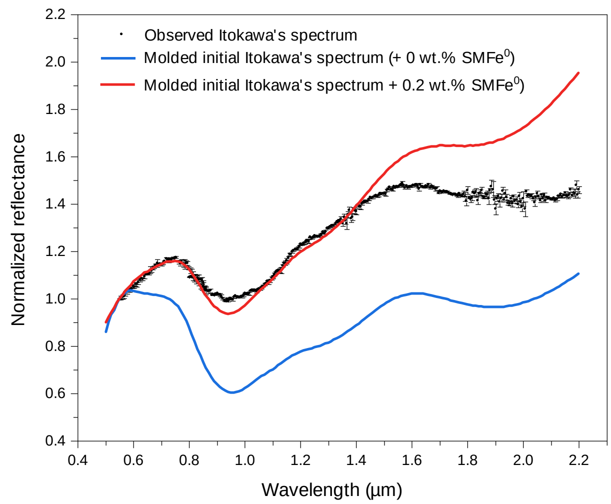

Fig. 1 | Estimation of Itokawa's SMFe^0 content. The observed Itokawa's spectrum best corresponds to 0.2 wt.% SMFe^0 content. Itokawa's observed spectrum is cited from Binzel et al. (2011)[1]. All the spectra are normalized at 0.55 μm.

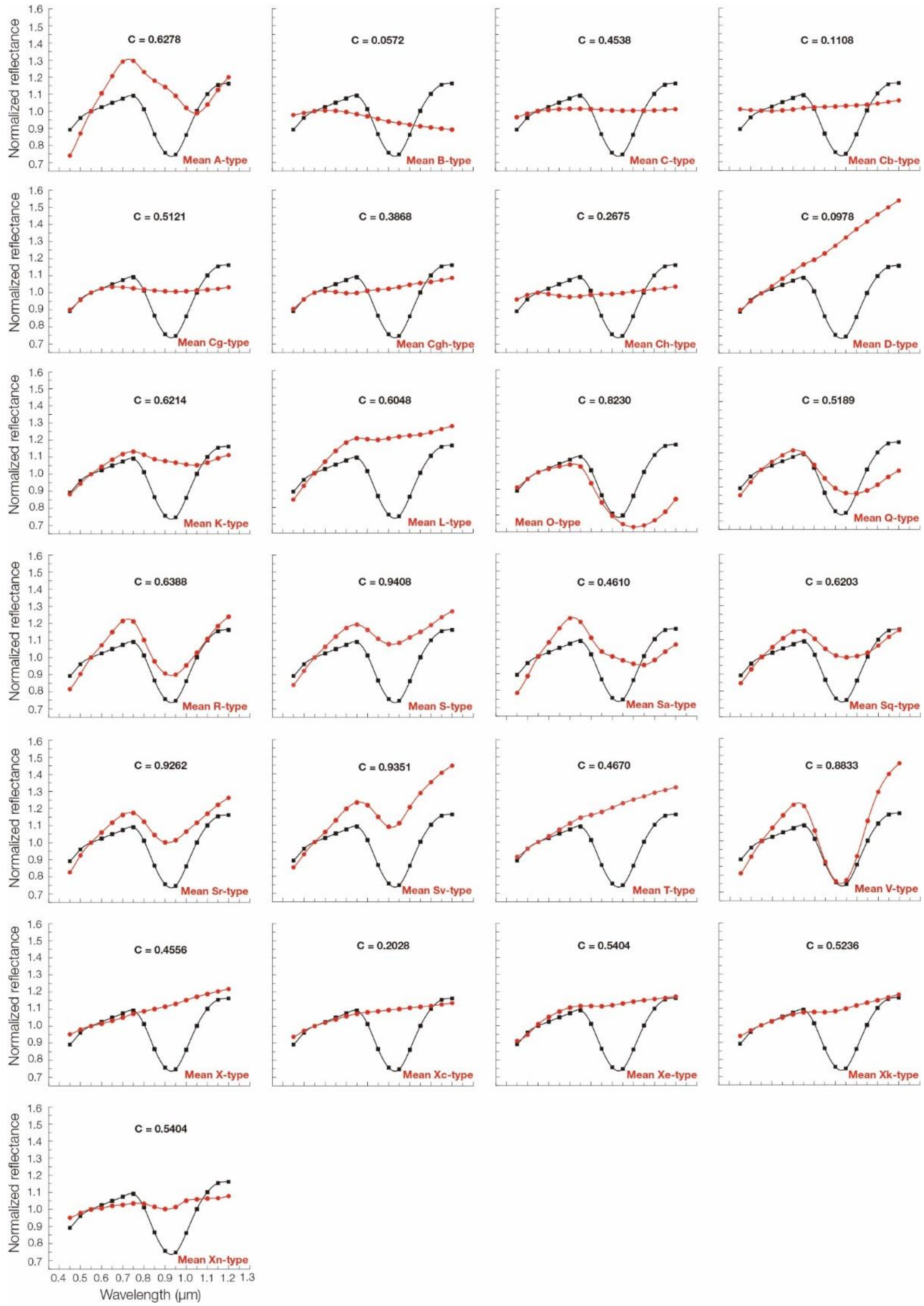

Fig. 2 | Comparison of Kamo‘oalewa’s spectrum with mean spectrum of each asteroid type. Kamo‘oalewa shows the highest confidence (C) as 0.9408 with mean spectrum of S-type, indicating that Kamo‘oalewa was best taxonomized as S-type. All the spectra are normalized at 0.55 μm.

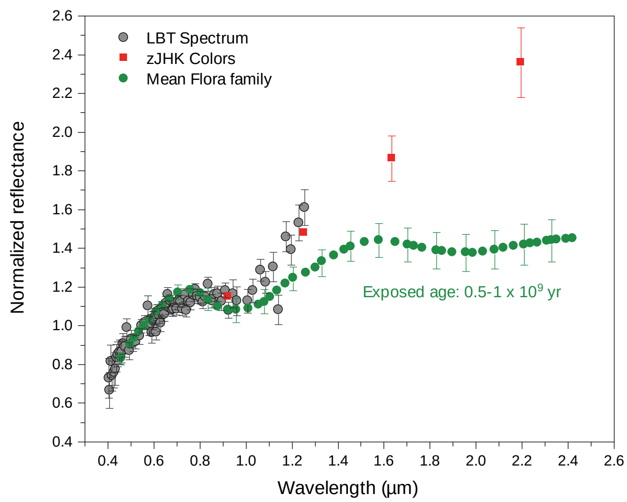

Fig. 3 | Comparison of Kamo'oalewa's spectrum with mean spectrum of Flora family. Kamo'oalewa shows a redder spectral slope than mean Flora family, suggesting that Kamo'oalewa has a higher SW degree than Flora family. Assuming that the SW rate at 1 AU area (Kamo'oalewa's position) is about 10 times that of the main belt area (position of Flora family), the SW timescale of Kamo'oalewa is estimated as at least $\sim 0.5-1 \times 10^8$ yr. All of the spectra are normalized at 0.55 μm. The mean spectrum data and exposure age of Flora family are cited from Vernazza et al. (2009)[2].

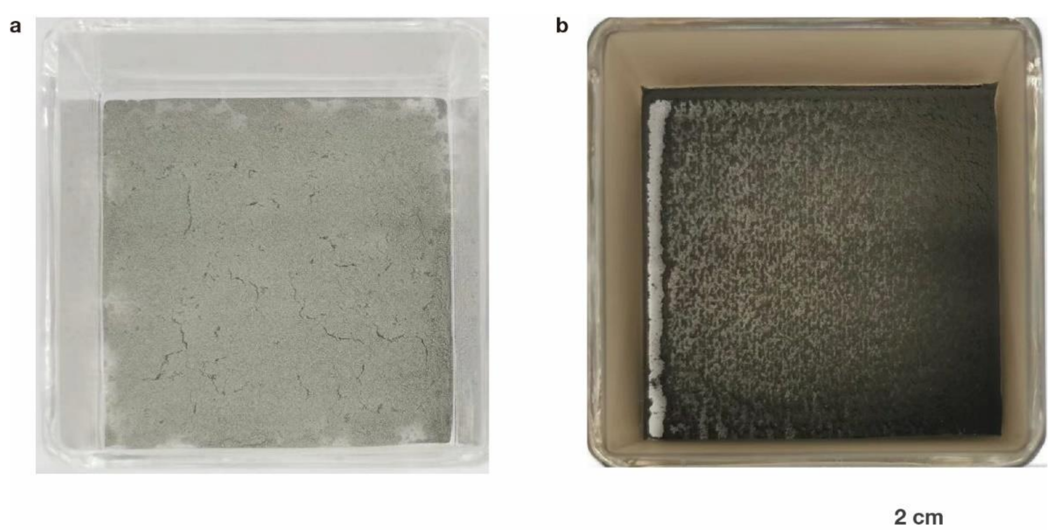

Fig. 4 | Photos of Kheneg Ljouâd's unpressed powder (size < 45 μm, mean size is 28.82 μm). a, Before laser irradiation. **b,** After laser irradiation. The powder significantly darkens after irradiation, namely, reflectance at 0.55 μm strongly decreases from 0.0303 to 0.085.

Measurement of mineral types and abundance of LL5/6 chondrite Kheneg Ljouâd

The mineral types and abundance of LL5/6 chondrite Kheneg Ljouâd were obtained by the TESCAN Integrated Mineral Analyzer (TIMA), which is located at the Nanjing Hongchuang Geological Exploration Technology Service Co., Ltd. This equipment is equipped with a MIRA-3 scanning electron microscope and four X-ray energy dispersive spectroscopy detectors to obtain the element information. As a result, this meteorite has 57.72781 vol.% olivine, 19.87455 vol.% orthopyroxene, 5.60751 vol.% diopside, 12.22511 vol.% plagioclase, 2.632 vol.% troilite, 0.04932 vol.% nickel-bearing troilite, 0.56471 vol.% tetrataenite, 0.7602 vol.% chromite, 0.03013 vol.% ilmenite, 0.12289 vol.% orthoclase, and 0.37811 vol.% apatite.

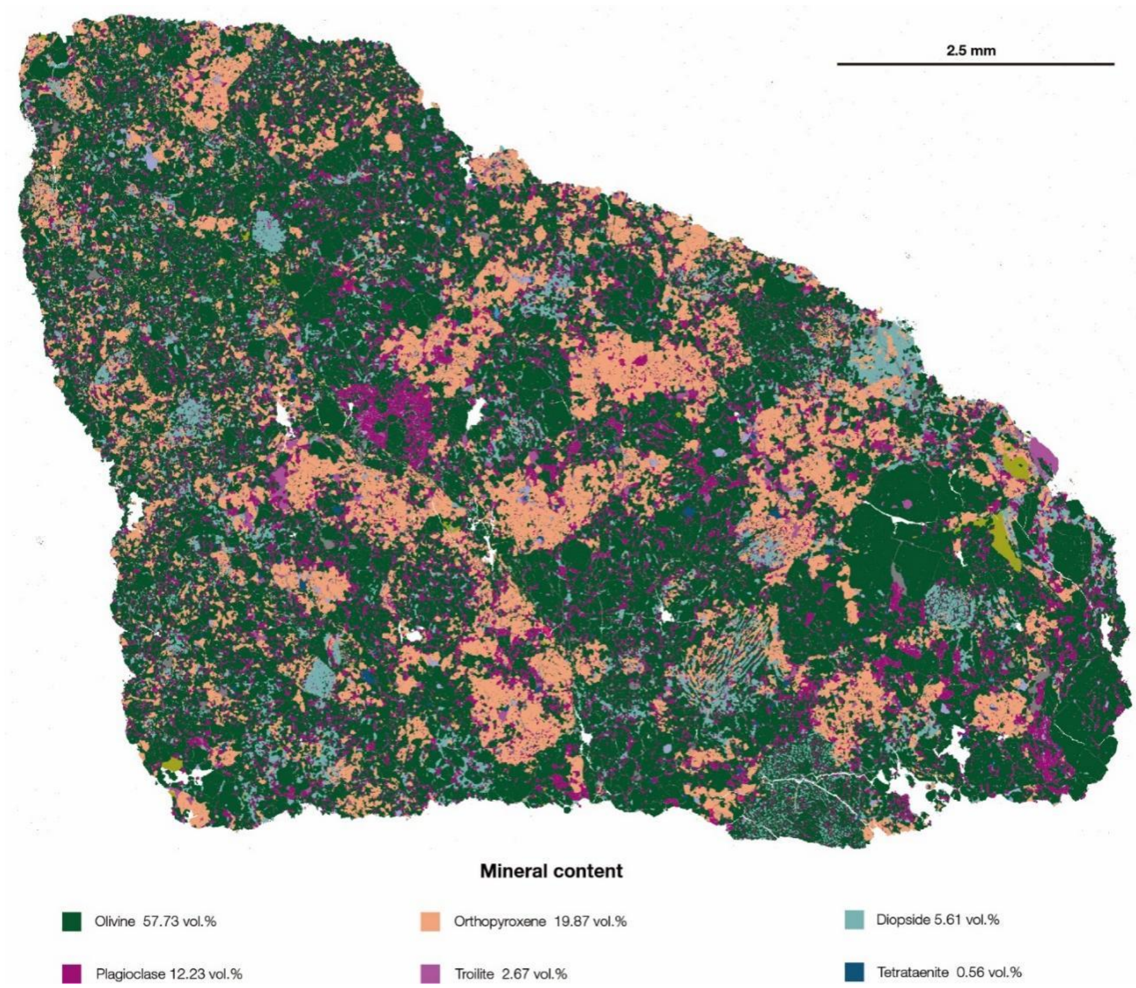

Fig. 5 | Mineral distribution and abundance of LL5/6 chondrite Kheneg Ljouâd obtained by the TIMA.

Spectral measurement of andesitic achondrite Erg Chech 002

A slab sample, that was ground by 120 grams Silicon-Carbide Sandpaper, was used to measure the reflectance spectra. The measurement was performed by the ASD FieldSpec 4 Hi-Res spectrometer installed at the Reflectance Spectroscopy Laboratory of Shandong University in Weihai, Shandong Province, China. This spectrometer is equipped with a 512-element silicon array detector (0.35–1.0 μm) and two Graded Index InGaAs detectors (1.001–1.8 μm, and 1.801–2.5 μm) to collect VIS-NIR reflectance spectral signals from 0.35 to 2.5 μm wavelength. Its light source is an ASD illuminator with a 57 W quartz-tungsten-halogen lamp, which can provide stable illumination over a 0.35–2.5 μm range for spectral measurement. The spectral resolution is 3 nm at 0.7 μm, and 8 nm at 1.4 μm and at 2.1 μm. The spectral sampling is 1.4 nm in the 0.35–1.0 μm region and 1.1 nm in the 1.001–2.5 μm region. Before measuring the spectra of sample, we first used a Spectralon Diffuse Reflectance Standard white plate for calibration and then set up the relative positions of the light source, white plate, and optical fiber probe as follows: (1) adjusting the position of the light source so that the light source is 30 cm away from the surface of standards, forming a uniform illumination spot with a diameter of approximately 6.3 cm; (2) adjusting the position of the detection fiber so that it is 5 mm from the surface of the white plate to ensure that all of the collected signals come from a circular area with a diameter of ~3 mm; (3) measuring the spectrum of each area of sample in turn. For each sample spot, the spectral signal was repeatedly collected 300 times and the average value was taken. The dark current was collected 100 times and averaged at each sample spot, then it was subtracted from the measurement. All the spectral measurements were performed with a phase angle of 30° (incident angle is 0°, and emission angle is 30°) in the air environment. We measured four different positions in total, namely, location 1, location 2, location 3, and location 4. Supplementary Fig. 6 shows the measured results.

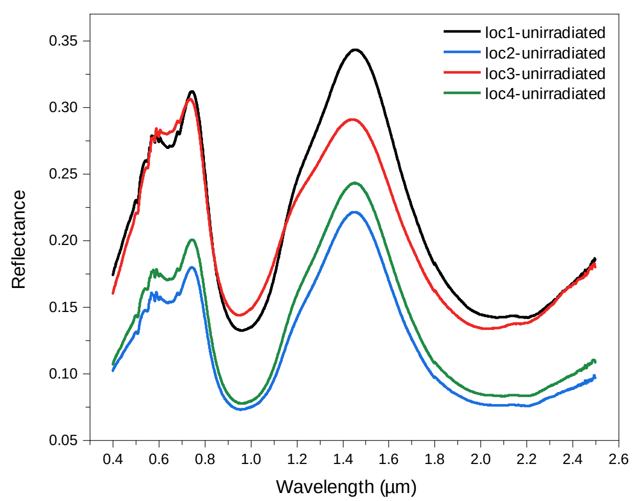

Fig. 6 | Reflectance spectra of andesitic achondrite Erg Chech 002 (slab). The spectra were measured in four different locations (loc1 to loc4) and at incidence angle $i = 0^{\circ}$, emission angle $e = 30^{\circ}$, and phase angle $g = 30^{\circ}$.

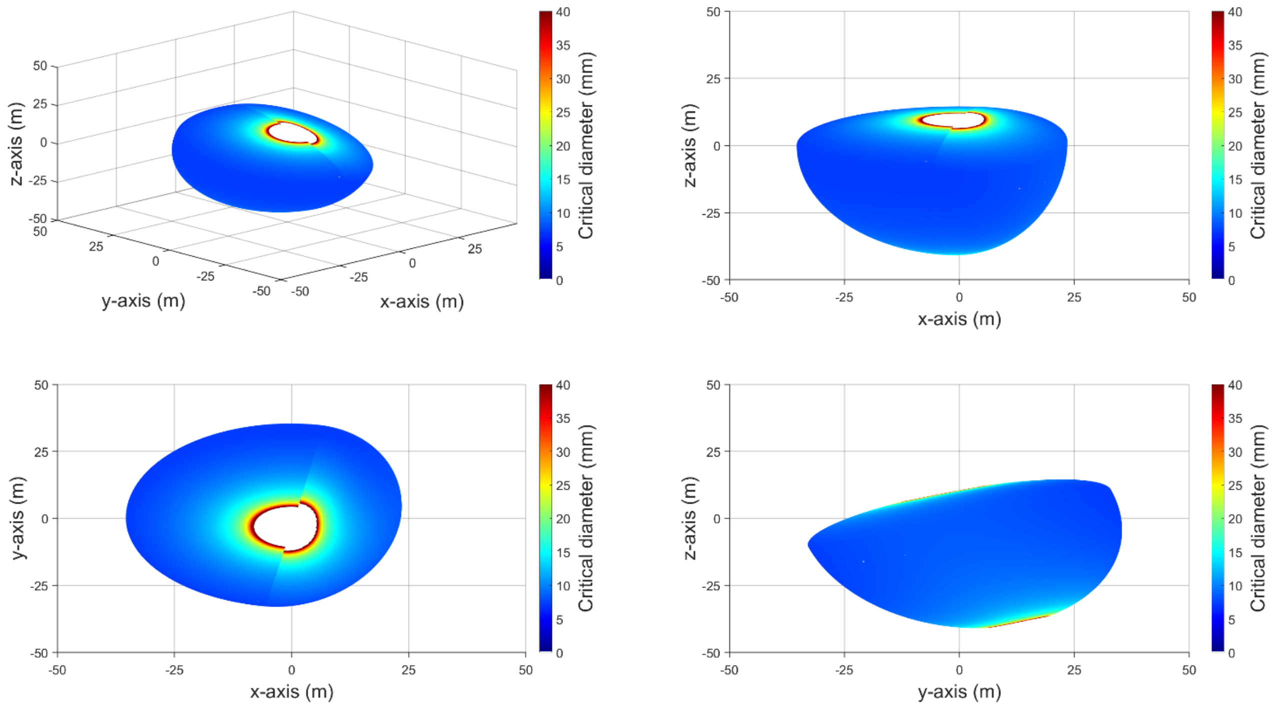

Fig. 7 Main view and three views of the global distribution of critical diameter of Kamo‘oalewa’s regolith rocks/grains. The red to blue colors represents the increasing critical diameter of the regolith rocks/grains. Regolith rocks/grains with a critical diameter $<$ 2 cm can stably remain on the 75.38% of the global surface area of Kamo‘oalewa. Two white zones (critical diameter of the regolith rocks/grains > 4 cm, occupying 2.83% of the global surface area) appear around the poles.

Table. 1 Background data of Fig. 1b.

Meteorite Types	Meteorite Names	Meteorite State	Spectral Data Sources (RELAB ID)	Band I Center (μm)	Band Area ratio	Reference
LL4	Benares (a)	<150 μm	MT-HYM-083	1.008	0.522	Dunn et al. (2010)[3]
LL4	Greenwell Springs	<150 μm	TB-TJM-075	0.991	0.512	Dunn et al. (2010)[3]
LL4	Hamlet	<150 μm	MT-HYM-075	0.980	0.561	Dunn et al. (2010)[3]
LL4	Witsand Farm	<150 μm	MT-HYM-076	1.004	0.457	Dunn et al. (2010)[3]
LL5	Aldsworth	<150 μm	MT-HYM-077	0.977	0.561	Dunn et al. (2010)[3]
LL5	Alta’ameem	<150 μm	MT-HYM-078	0.986	0.435	Dunn et al. (2010)[3]
LL5	Olivenza	<150 μm	MT-HYM-085	1.012	0.387	Dunn et al. (2010)[3]
LL5	Paragould	<150 μm	MT-HYM-079	0.985	0.409	Dunn et al. (2010)[3]

LL5	Tuxtuac	<150 µm	MT-HYM-080	1.035	0.310	Dunn et al. (2010)[3]
LL6	Bandong	<150 µm	TB-TJM-067	1.001	0.274	Dunn et al. (2010)[3]
LL6	Cherokee Springs	<150 µm	TB-TJM-075	0.989	0.406	Dunn et al. (2010)[3]
LL6	Karatu	<75 µm	TB-TJM-077	1.006	0.311	Dunn et al. (2010)[3]
LL6	Saint-Séverin	<150 µm	TB-TJM-145	1.003	0.269	Dunn et al. (2010)[3]
LL5/6	Kheneg Ljouâd	<45 µm	This study	0.990	0.298	This study
L4	Attarra	<150 µm	TB-TJM-065	0.957	0.726	Dunn et al. (2010)[3]
L4	Bald Mountain	<150 µm	TB-TJM-102	0.929	0.960	Dunn et al. (2010)[3]
L4	Rio Negro	<150 µm	TB-TJM-081	0.953	0.813	Dunn et al. (2010)[3]
L4	Rupota	<150 µm	TB-TJM-121	0.955	0.582	Dunn et al. (2010)[3]
L5	Ausson	<150 µm	MT-HYM-084	0.930	1.031	Dunn et al. (2010)[3]
L5	Blackwell	<150 µm	MT-HYM-081	0.955	0.526	Dunn et al. (2010)[3]
L5	Cilimus	<150 µm	MT-HYM-082	0.950	0.515	Dunn et al. (2010)[3]
L5	Guibga	<150 µm	TB-TJM-134	0.962	0.633	Dunn et al. (2010)[3]
L5	Mabwe-Khoywa	<150 µm	TB-TJM-107	0.954	0.744	Dunn et al. (2010)[3]
L5	Messina	<150 µm	TB-TJM-099	0.959	0.595	Dunn et al. (2010)[3]
L6	Apt	<150 µm	TB-TJM-064	0.963	0.511	Dunn et al. (2010)[3]
L6	Aumale	<150 µm	TB-TJM-101	0.960	0.614	Dunn et al. (2010)[3]
L6	Kunashak	<150 µm	TB-TJM-139	0.972	0.518	Dunn et al. (2010)[3]
L6	Kyushu	<150 µm	TB-TJM-140	0.970	0.544	Dunn et al. (2010)[3]
L6	New Concord	<150 µm	TB-TJM-130	0.960	0.606	Dunn et al. (2010)[3]
H4	Farmville	<150 µm	TB-TJM-128	0.939	0.789	Dunn et al. (2010)[3]
H4	Forest Vale	<75 µm	TB-TJM-093	0.937	0.800	Dunn et al. (2010)[3]
H4	Kabo	<150 µm	TB-TJM-136	0.939	0.915	Dunn et al. (2010)[3]
H4	Marilia	<150 µm	TB-TJM-078	0.934	0.851	Dunn et al. (2010)[3]
H4	São Jose do Rio Preto	<150 µm	TB-TJM-082	0.942	0.992	Dunn et al. (2010)[3]
H5	Allegan	rock	TB-TJM-104	0.930	1.068	Dunn et al. (2010)[3]
H5	Ehole	<150 µm	TB-TJM-074	0.940	0.999	Dunn et al. (2010)[3]
H5	Itapicuru-Mirim	<150 µm	TB-TJM-097	0.944	0.878	Dunn et al. (2010)[3]
H5	Lost City	<150 µm	TB-TJM-129	0.940	0.857	Dunn et al. (2010)[3]
H5	Primbram	<150 µm	TB-TJM-143	0.940	0.857	Dunn et al. (2010)[3]
H5	Schenectady	<150 µm	TB-TJM-083	0.937	0.786	Dunn et al. (2010)[3]
H5	Uberaba	<150 µm	TB-TJM-085	0.945	0.881	Dunn et al. (2010)[3]
H6	Andura	<75 µm	TB-TJM-088	0.927	0.889	Dunn et al. (2010)[3]
H6	Bustura	<150 µm	TB-TJM-069	0.936	0.795	Dunn et al. (2010)[3]
H6	Canon City	<150 µm	TB-TJM-131	0.953	0.752	Dunn et al. (2010)[3]

H6	Chiang Khan	<150 µm	TB-TJM-132	0.946	0.846	Dunn et al. (2010)[3]
H6	Guarena	<150 µm	TB-TJM-094	0.938	0.748	Dunn et al. (2010)[3]
H6	Ipiranga	<150 µm	TB-TJM-135	0.939	0.835	Dunn et al. (2010)[3]
Ureilite	ALH A77257	<75 µm	c1ph27	0.932	0.4	Cloutis et al. (2010)[4]
Ureilite	ALH A81101	<75 µm	c1ph30	0.947	0.23	Cloutis et al. (2010)[4]
Ureilite	ALH 82130	<75 µm	c1ph21	0.938	0.88	Cloutis et al. (2010)[4]
Ureilite	DaG 319	<75 µm	c1ph39	0.957	0.22	Cloutis et al. (2010)[4]
Ureilite	EET 87517	<75 µm	c1ph24	0.924	0.44	Cloutis et al. (2010)[4]
Ureilite	EET 87720	<75 µm	c1ph37	0.920	0.34	Cloutis et al. (2010)[4]
Ureilite	EET 96042	<75 µm	c1ph31	0.949	0.21	Cloutis et al. (2010)[4]
Ureilite	GRA 95205	<75 µm	c1ph23	0.924	0.50	Cloutis et al. (2010)[4]
Ureilite	GRO 95575	<75 µm	c1ph25	0.950	0.35	Cloutis et al. (2010)[4]
Ureilite	Kenna	<75 µm	c1ph38	0.962	0.38	Cloutis et al. (2010)[4]
Ureilite	LEW 85440	<75 µm	c1ph22	0.938	0.35	Cloutis et al. (2010)[4]
Ureilite	MET 01085	<75 µm	c1ph40	0.923	0.87	Cloutis et al. (2010)[4]
Ureilite	Novo Urei	<75 µm	c1ph28	0.960	0.75	Cloutis et al. (2010)[4]
Ureilite	PCA 82506	<75 µm	c1ph26	0.948	0.29	Cloutis et al. (2010)[4]
Ureilite	Y-791538	<75 µm	c1ph19	0.929	0.38	Cloutis et al. (2010)[4]
Acapulcoites	Acapulco	<125 µm	TB-TJM-043	0.923	0.930	Lucas et al. (2019)[5]
Acapulcoites	MET 01212	<125 µm	MT-JPE-301-T	0.920	0.887	Lucas et al. (2019)[5]
Acapulcoites	Dhofar 125	<125 µm	MT-JPE-304-T	0.923	0.766	Lucas et al. (2019)[5]
Acapulcoites	NWA 725	<125 µm	MT-JPE-305-T	0.913	0.986	Lucas et al. (2019)[5]
Acapulcoites	NWA 2871	<125 µm	MT-JPE-306-T	0.930	0.540	Lucas et al. (2019)[5]

Lodranites	Lodran	rock	TB-TJM-041	0.920	0.944	Lucas et al. (2019)[5]
Lodranites	LAR 06605	<125 μm	MT-JPE-300-T	0.927	0.848	Lucas et al. (2019)[5]
Lodranites	MAC 88177	<125 μm	MT-JPE-302-T	0.940	0.605	Lucas et al. (2019)[5]
Lodranites	NWA 7674	<125 μm	MT-JPE-310-T	0.930	0.825	Lucas et al. (2019)[5]
Winonaites	NWA 1643	rock	c1mt09	0.920	0.433	This study
Winonaites	NWA 4024	<125 μm	c1mt307t	0.920	0.166	This study
Winonaites	NWA 4024	slab	camt307	0.940	0.101	This study
Brachinite	Reid 013	chip	c1mt52	1.050	0.050	This study
Brachinite	EET 99402	fine powder	c1mt88	1.070	0.037	This study
Brachinite	EET 99402	<45 μm	c1mt329	1.070	0.011	This study
Brachinite	RaS 309	<45 μm	c1mt345	1.050	0.031	This study
Brachinite	NWA 7297	<45 μm	c1mt346	1.030	0.079	This study
Brachinite	EET 99402	<125 μm	c1tb58	1.080	0.022	This study
Brachinite	Brachina	<45 μm	camt49	1.045	0.001	This study
Howardite	Bialystok	150 μm		0.937	1.641	Moskovitz et al. (2010)[6]
Howardite	Binda	25 μm		0.928	1.693	Moskovitz et al. (2010)[6]
Howardite	Bununu	25 μm		0.928	1.474	Moskovitz et al. (2010)[6]
Howardite	EET 83376	25 μm		0.934	1.784	Moskovitz et al. (2010)[6]
Howardite	EET 87503	25 μm		0.929	1.619	Moskovitz et al. (2010)[6]
Howardite	EET 87513	25 μm		0.932	1.469	Moskovitz et al. (2010)[6]
Howardite	Frankfort	25 μm		0.927	1.764	Moskovitz et al. (2010)[6]
Howardite	GRO 95535	25 μm		0.929	1.671	Moskovitz et al. (2010)[6]
Howardite	GRO 95574	125 μm		0.929	1.757	Moskovitz et al. (2010)[6]
Howardite	Kapoeta	25 μm		0.928	1.372	Moskovitz et al. (2010)[6]
Howardite	Le Teilleul	25 μm		0.928	1.935	Moskovitz et al. (2010)[6]
Howardite	Pavlovka	Chip		0.921	1.978	Moskovitz et al. (2010)[6]

Howardite	Petersburg	25 μm		0.934	1.830	Moskovitz et al. (2010)[6]
Howardite	QUE 94200	25 μm		0.921	1.862	Moskovitz et al. (2010)[6]
Howardite	QUE 97001	125 μm		0.924	2.079	Moskovitz et al. (2010)[6]
Howardite	Y-7308	25 μm		0.927	1.697	Moskovitz et al. (2010)[6]
Howardite	Y-790727	25 μm		0.931	1.910	Moskovitz et al. (2010)[6]
Howardite	Y-791573	25 μm		0.926	1.802	Moskovitz et al. (2010)[6]
Eucrite	A87272	25 μm		0.941	1.224	Moskovitz et al. (2010)[6]
Eucrite	A881819	25 μm		0.931	1.560	Moskovitz et al. (2010)[6]
Eucrite	ALH 78132	45 μm		0.933	2.138	Moskovitz et al. (2010)[6]
Eucrite	ALH 85001	25 μm		0.925	1.552	Moskovitz et al. (2010)[6]
Eucrite	ALH A76005	25 μm		0.935	1.726	Moskovitz et al. (2010)[6]
Eucrite	ALH A81001	45 μm		0.937	2.799	Moskovitz et al. (2010)[6]
Eucrite	ALH A81011	125 μm		0.951	1.336	Moskovitz et al. (2010)[6]
Eucrite	ALH A85001	1000 μm		0.932	1.680	Moskovitz et al. (2010)[6]
Eucrite	Bereba	25 μm		0.941	1.706	Moskovitz et al. (2010)[6]
Eucrite	Bouvante	25 μm		0.943	2.241	Moskovitz et al. (2010)[6]
Eucrite	BTN 00300	45 μm		0.947	0.942	Moskovitz et al. (2010)[6]
Eucrite	Cachari	25 μm		0.940	1.480	Moskovitz et al. (2010)[6]
Eucrite	EET 83251	1000 μm		0.937	2.191	Moskovitz et al. (2010)[6]
Eucrite	EET 87520	45 μm		0.951	1.112	Moskovitz et al.

						(2010)[6]
Eucrite	EET 87542	25 µm		0.940	1.346	Moskovitz et al. (2010)[6]
Eucrite	EET 90020	25 µm		0.941	0.987	Moskovitz et al. (2010)[6]
Eucrite	EET 92003	125 µm		0.933	1.659	Moskovitz et al. (2010)[6]
Eucrite	EET A79005	25 µm		0.934	2.003	Moskovitz et al. (2010)[6]
Eucrite	EET A79006	125 µm		0.935	1.934	Moskovitz et al. (2010)[6]
Eucrite	EET A790B	1000 µm		0.937	2.007	Moskovitz et al. (2010)[6]
Eucrite	GRO 95533	25 µm		0.941	1.458	Moskovitz et al. (2010)[6]
Eucrite	Ibitra	25 µm		0.940	1.134	Moskovitz et al. (2010)[6]
Eucrite	Jonzac	25 µm		0.939	1.795	Moskovitz et al. (2010)[6]
Eucrite	Juvinas	25 µm		0.936	1.605	Moskovitz et al. (2010)[6]
Eucrite	LEW 85303	25 µm		0.945	1.570	Moskovitz et al. (2010)[6]
Eucrite	LEW 87004	25 µm		0.934	1.784	Moskovitz et al. (2010)[6]
Eucrite	MAC 02522	45 µm		0.970	0.831	Moskovitz et al. (2010)[6]
Eucrite	MET 01081	45 µm		0.939	1.2518	Moskovitz et al. (2010)[6]
Eucrite	Millbillillie	25 µm		0.938	1.361	Moskovitz et al. (2010)[6]
Eucrite	Moore County	25 µm		0.938	1.389	Moskovitz et al. (2010)[6]
Eucrite	NWA 011	25 µm		0.950	0.919	Moskovitz et al. (2010)[6]
Eucrite	Padvarninkai	25 µm		0.939	1.485	Moskovitz et al. (2010)[6]
Eucrite	Pasamonte	25 µm		0.939	1.545	Moskovitz et al. (2010)[6]

Eucrite	PCA 82501	125 µm		0.943	1.906	Moskovitz et al. (2010)[6]
Eucrite	PCA 82502	25 µm		0.941	2.216	Moskovitz et al. (2010)[6]
Eucrite	PCA 91006	125 µm		0.942	1.359	Moskovitz et al. (2010)[6]
Eucrite	PCA 91007	125 µm		0.943	2.138	Moskovitz et al. (2010)[6]
Eucrite	PCA 91078	45 µm		0.955	1.784	Moskovitz et al. (2010)[6]
Eucrite	Serra de Mage	25 µm		0.931	1.512	Moskovitz et al. (2010)[6]
Eucrite	Stannern	25 µm		0.938	1.917	Moskovitz et al. (2010)[6]
Eucrite	Y-74450	25 µm		0.934	1.362	Moskovitz et al. (2010)[6]
Eucrite	Y-75011	1000 µm		0.947	1.238	Moskovitz et al. (2010)[6]
Eucrite	Y-791186	1000 µm		0.949	1.482	Moskovitz et al. (2010)[6]
Eucrite	Y-792510	25 µm		0.942	1.337	Moskovitz et al. (2010)[6]
Eucrite	Y-792769	25 µm		0.941	1.659	Moskovitz et al. (2010)[6]
Eucrite	Y-793591	25 µm		0.939	1.857	Moskovitz et al. (2010)[6]
Eucrite	Y-82082	25 µm		0.947	1.631	Moskovitz et al. (2010)[6]
Eucrite	Y-980318	75 µm		0.940	1.486	Moskovitz et al. (2010)[6]
Diogenite	EET A79002	25 µm		0.917	1.758	Moskovitz et al. (2010)[6]
Diogenite	Ellemeet	25 µm		0.920	1.901	Moskovitz et al. (2010)[6]
Diogenite	Johnstown	25 µm		0.914	1.509	Moskovitz et al. (2010)[6]
Diogenite	LAP 91900	1000 µm		0.925	1.970	Moskovitz et al. (2010)[6]
Diogenite	Roda	Chip		0.923	1.988	Moskovitz et al.

						(2010)[6]
Diogenite	Shalka	Chip		0.918	2.204	Moskovitz et al. (2010)[6]
Diogenite	Tatahouine	Chip		0.920	1.862	Moskovitz et al. (2010)[6]
Diogenite	Y-74013	25 μm		0.920	1.763	Moskovitz et al. (2010)[6]
Diogenite	Y-75032	25 μm		0.926	1.704	Moskovitz et al. (2010)[6]
Andesitic achondrite	Erg Chech 002	slab	This study	0.961	1.316	This study
Andesitic achondrite	Erg Chech 002	slab	This study	0.976	1.405	This study
Andesitic achondrite	Erg Chech 002	slab	This study	0.948	1.429	This study
Andesitic achondrite	Erg Chech 002	slab	This study	0.975	1.405	This study
Pallasites	Y-8451	unknown	c2mb39	1.045	0.013	This study
Pallasites	Imilac	slab	c2mb41	1.055	0.102	This study
Pallasites	Imilac	slab	c4mb41	1.095	0.007	This study
Pallasites	Esquel	<25 μm	camb43	1.055	0.030	This study
Pallasites	Esquel	**75-125** μm	cdmb43	1.065	0.056	This study
Pallasites	Esquel	125-250 μm	cemb43	1.075	0.023	This study
Pallasites	Esquel	<25 μm	chmb43	1.055	0.023	This study
Pallasites	Esquel	45-75 μm	cjmb43	1.055	0.018	This study
Mesosiderites	Estherville	rock	c1tb148	0.930	2.173	This study
Mesosiderites	Vaca Muerta	rock	c1tb149	0.930	1.425	This study
Mesosiderites	Lamont	rock	c1tb150	0.930	2.840	This study
Mesosiderites	EET 87500	<125 μm	c1tb159	0.930	1.659	This study
Mesosiderites	EET 92001	<125 μm	c1tb162	0.930	1.586	This study
Mesosiderites	Barea	slab	c3mb33	0.915	1.995	This study
Mesosiderites	Barea	slab	c4mb33	0.925	1.602	This study

Note: The RELAB ID in Dunn et al. (2010)[3] and Lucas et al. (2019)[5] refers to Sample ID, in Cloutis et al. (2010)[4] and this study refer to Spectral ID. Four spectral data of andesitic achondrite Erg Chech 002 (slab) (Supplementary Fig. 4) were measured and first published in this study.

Table. 2 Background data of Fig. 2.

Asteroid Types	Asteroid Numbers	Asteroid Names	VIS-NIR Spectral Slope	Spectral Files
		NEAs		
A	1951	Lick	1.20528	a001951.sp72
A	6053	1993 BW_3	0.33926	a006053.sp233.txt
B	1508	Kemi	-0.03278	a001508.sp28
B	2100	Ra-Shalom	-0.01034	a002100.sp222.txt
B	3200	Phaethon	-0.10736	a003200.sp239.txt
B	17511	1992 QN	0.00290	a017511.sp239.txt
B	25330	1999 KV_4	-0.05228	a025330.sp19
C	3833	Calingasta	0.06434	a003833.sp92
C	65679	1989 UQ	0.02348	a065679.sp94
Ch	2099	Öpik	0.11265	a002099.sp45
D	3552	Don Quixote	0.98782	a003552.sp85
D	17274	2000 LC_{16}	0.4667	a017274.sp245n2.txt
K	3199	Nefertiti	0.23164	a003199.sp36
L	7304	Namiki	0.4867	a007304.sp59
L	85989	1999 JD_6	0.11559	a085989.sp92
L	98943	2001 CC_{21}	0.45743	au2001CC21.sp33
L	138911	2001 AE_2	0.33747	a138911.sp265.txt
L	385186	1994 AW_1	0.28726	a385186.sp209.txt
L	506459	2002 AL_{14}	0.58147	au2002AL14.sp27
Q	3753	Cruithne	0.2011	a003753.sp45
Q	4183	Cuno	0.03337	a004183.sp103
Q	4688	1980 WF	0.17757	a004688.sp03
Q	5143	Heracles	0.10482	a005143.sp287.txt
Q	5660	1974 MA	0.13927	a005660.sp43
Q	7336	Saunders	0.01882	a007336.sp93
Q	7341	1991 VK	0.254	a007341.sp224.txt
Q	152931	2000 EA_{107}	0.07633	a152931.sp89
Q	219071	1997 US_9	0.1246	a219071.sp104
Q	422686	2000 AC_6	0.16728	a422686.sp206.txt
S	719	Albert	0.23774	a000719.sp08
S	887	Alinda	0.05478	a000887.sp111
S	1065	Amundsenia	0.28105	a001065.sp37
S	1131	Porzia	0.24576	a001131.sp28
S	1620	Geographos	0.1875	a001620.sp212.txt
S	1640	Nemo	0.20152	a001640.sp37

S	1865	Cerberus	0.1518	a001865.sp75
S	2078	Nanking	0.10915	a002078.sp92
S	3674	Erbisbühl	0.12581	a003674.sp92
S	5626	1991 FE	0.22403	a005626.sp84
S	5836	1993 MF	0.26241	a005836.sp221.txt
S	6047	1991 TB_1	0.17093	a006047.sp45
S	6386	Keithnoll	0.28876	a006386.sp36
S	6585	O'Keefe	0.15382	a006585.sp55
S	7482	1994 PC_1	0.20433	a007482.sp72
S	7822	1991 CS	0.40322	a007822.sp216
S	9400	1994 TW_1	0.16752	a009400.sp215.txt
S	11500	Tomaiyowit	0.2512	a011500.sp65
S	15745	Yuliya	0.36967	a15745.sp242.txt
S	16834	1997 WU_{22}	0.26861	a016834.sp84
S	20790	2000 SE_{45}	0.08636	a020790.sp03
S	22771	1999 CU_3	0.30409	a022771.sp26
S	35396	1997 XF_{11}	0.03994	a035396.sp217.txt
S	36017	1999 ND_{43}	0.17363	a036017.sp203.txt
S	85990	1999 JV_6	0.22915	a085990.sp215.txt
S	100756	1998 FM_5	0.28683	a100756.sp287.txt
S	189040	2000 MU_1	0.05713	a189040.sp279n1.txt
Sw	433	Eros	0.37964	a000433.sp245n2.txt
Sw	1139	Atami	0.31543	a001139.sp29
Sw	1204	Renzia	0.33589	a001204.sp37
Sw	1627	Ivar	0.30518	a001627.sp290n1.txt
Sw	1866	Sisyphus	0.39781	a001866.sp56
Sw	1916	Boreas	0.4274	a001916.sp07
Sw	1943	Anteros	0.33296	a001943.sp09
Sw	1980	Tezcatlipoca	0.46433	a001980.sp55
Sw	2074	Shoemaker	0.52025	a002074.sp25
Sw	2335	James	0.28533	a002335.sp46
Sw	3352	McAuliffe	0.29979	a003352.sp106
Sw	24475	2000 VN_2	0.38009	a024475.sp05
Sw	163000	2001 SW_{169}	0.04148	a163000.sp212.txt
Sa	5261	Eureka	0.44726	a005261.sp41
Sq	699	Hela	0.15334	a000699.sp35
Sq	1374	Isora	0.15982	a001374.sp28
Sq	1685	Toro	0.23463	a001685.sp217.txt

Sq	2063	Bacchus	0.0749	a002063.sp41
Sq	2340	Hathor	0.05534	a002340.sp203.txt
Sq	4179	Toutatis	0.15312	a004179.sp228.txt
Sq	4197	1982 TA	0.09432	a004197.sp25
Sq	7358	Oze	0.07757	a007358.sp100
Sq	19356	1997 GH_3	0.13144	a019356.sp03
Sq	31345	1998 PG	0.17251	a31345.sp246n1.txt
Sq	35107	1991 VH	0.25816	a035107.sp20
Sq	86819	2000 GK_{137}	0.18331	au2000GK137.sp02
Sq	99942	Apophis	0.19398	au2004MN4.sp35
Sq	137799	1999 YB	0.11538	a137799.sp103
Sq	194386	2001 VG_5	0.13283	a194386.sp214.txt
Sq	203015	1999 YF_3	0.23867	a203015.sp263n1.txt
Sqw	512	Taurinensis	0.3281	a000512.sp32
Sqw	2064	Thomsen	0.28628	a002064.sp52
Sqw	3102	Krok	0.27678	a003102.sp02
Sqw	3122	Florence	0.39737	a003122.sp27
Sqw	3288	Seleucus	0.36366	a003288.sp99
Sr	1036	Ganymed	0.20863	a001036.sp290n1.txt
Sr	1565	Lemaître	0.08526	a001565.sp36
Sr	4558	Janesick	0.15523	a004558.sp29
Sr	5587	1990 SB	0.06686	a005587.sp224.txt
Sr	5817	Robertfrazer	0.19789	a005817.sp31
Sr	16960	1998 QS_{52}	-0.00435	a016960.sp74
Sr	99907	1989 VA	0.20565	au1989VA.sp19
Sr	137062	1998 WM	0.18233	au1998WM.sp19
Sr	138524	2000 OJ_8	0.11126	a138524.sp102
Srw	3635	Kreutz	0.32573	a003635.sp47
Srw	3858	Dorchester	0.27082	a003858.sp28
Srw	4142	Dersu-Uzala	0.85057	ref [06]
Srw	4954	Eric	0.32153	a004954.sp61
Srw	53435	1999 VM_{40}	0.44258	a053435.sp274n1.txt
Srw	85818	1998 XM_4	0.31514	a085818.sp91
Sv	5392	Parker	0.22192	a005392.sp95
V	3908	Nyx	-0.01697	a003908.sp30
X	153201	2000 WO_{107}	0.29689	a153201.sp278n1.txt
Xe	132	Aethra	0.1142	a000132.sp44
Xe	3103	Eger	0.26716	a003103.sp289.txt

Xe	4660	Nereus	0.1044	a004660.sp291.txt
Xk	3691	Bede	0.14769	a003691.sp68
MBAs				
A	246	Asporina	0.60629	a000246.sp37
A	354	Eleonora	0.51649	a000354.dm02.txt
A	863	Benkoela	1.02849	a000863.sp76
B	2	Pallas	-0.08015	a000002.sp89
B	1508	Kemi	-0.03278	a001508.sp28
B	3200	Phaethon	-0.10736	a003200.sp239.txt
C	1	Ceres	-0.01071	a000001.sp41
C	10	Hygiea	-0.03617	a000010.sp111
C	24	Themis	0.01601	a000024.sp45
C	52	Europa	0.1469	a000052.sp52
C	76	Freia	0.22841	a000076.sp44
C	90	Antiope	0.15904	a000090.sp44
C	128	Nemesis	0.15085	a000128.sp263n1.txt
Cb	191	Kolga	0.16166	a000191.sp38
Cb	210	Isabella	0.07337	a000210.sp47
Cb	785	Zwetana	0.16602	a000785.sp41
Cg	175	Andromache	0.10724	a000175.sp47
Cgh	38	Leda	0.17371	a000038.sp100
Cgh	51	Nemausa	0.22141	a000051.sp29
Cgh	54	Alexandra	0.13206	a000054.sp259n2.txt
Cgh	706	Hirundo	0.20732	a000706.sp49
Cgh	776	Berbericia	0.13156	a000776.sp38
Cgh	1300	Marcelle	0.15541	a001300.sp56
Cgh	2378	Pannekoek	0.05804	a002378.sp40.txt
Ch	13	Egeria	0.0928	a000013.sp41
Ch	19	Fortuna	0.20157	a000019.sp49
Ch	34	Circe	0.09265	a000034.sp28
Ch	41	Daphne	0.07113	a000041.sp84
Ch	48	Doris	0.0165	a000048.sp45
Ch	50	Virginia	0.03168	a000050.sp265.txt
Ch	58	Concordia	0.07816	a000058.sp265.txt
Ch	66	Maja	0.10663	sp [048]
Ch	78	Diana	0.12491	a000078.sp46
Ch	105	Artemis	0.12845	a000105.sp25
Ch	111	Ate	0.00502	a000111.sp31

Ch	266	Aline	0.10456	a000266.sp44
Ch	345	Tercidina	0.11947	a000345.sp45
Ch	2099	Öpik	0.11265	a002099.sp45
D	269	Justitia	1.39277	a000269.sp40.txt
D	279	Thule	0.6119	a000279.sp35
D	570	Kythera	0.49883	a000570.sp28
D	908	Buda	0.81727	a000908.sp53
D	944	Hidalgo	0.72672	a000944.sp31
D	1542	Schalén	0.83058	a001542.sp39
D	2246	Bowell	0.63755	a002246.sp39
D	3248	Farinella	0.59193	a003248.sp39
D	3317	Paris	0.58063	a003317.sp50
K	15	Eunomia	0.14049	a000015.sp28
K	114	Kassandra	0.24911	a000114.sp52
K	131	Vala	0.17203	a000131.sp53
K	3199	Nefertiti	0.23164	a003199.sp36
L	234	Barbara	0.42228	a000234.sp57
L	236	Honoria	0.27009	a000236.sp50
L	679	Pax	0.19109	a000679.sp89
L	1332	Marconia	0.1338	a001332.sp42
O	3628	Božněmcová	0.04891	sp [050]
Q	3753	Cruithne	0.2011	a003753.sp45
Q	4688	1980 WF	0.17757	a004688.sp03
Q	5143	Heracles	0.10482	a005143.sp287.txt
Q	5660	1974 MA	0.13927	a005660.sp43
Q	7341	1991 VK	0.254	a007341.sp224.txt
S	5	Astraea	0.19655	a000005.sp28
S	7	Iris	0.17956	a000007.sp28
S	14	Irene	0.21363	a000014.sp25
S	17	Thetis	0.30848	a000017.sp96
S	20	Massalia	0.24574	a000020.sp96
S	25	Phocaea	0.35887	a000025.sp94
S	26	Proserpina	0.22945	a000026.sp92
S	27	Euterpe	0.27512	a000027.sp31
S	29	Amphitrite	0.18642	a000029.sp92
S	30	Urania	0.30259	a000030.sp92
S	37	Fides	0.19858	a000037.sp94
S	40	Harmonia	0.15335	a000040.sp32

S	57	Mnemosyne	0.22072	a000057.sp92
S	61	Danaë	0.2081	a000061.sp94
S	67	Asia	0.15598	a000067.sp111
S	82	Alkmene	0.12482	a000082.sp92
S	101	Helena	0.21507	a000101.sp57
S	103	Hera	0.26641	a000103.sp92
S	119	Althaea	0.39973	a000119.sp92
S	158	Koronis	0.22747	a000158.sp94
S	264	Libussa	0.25464	a000264.sp41
S	288	Glauke	0.15635	a000288.sp92
S	371	Bohemia	0.16713	a000371.sp92
S	389	Industria	0.15516	a000389.sp94
S	403	Cyane	0.2745	a000403.sp93
S	532	Herculina	0.21433	a000532.sp76
S	631	Philippina	0.25752	a000631.sp101
S	699	Hela	0.15334	a000699.sp35
S	719	Albert	0.23774	a000719.sp08
S	793	Arizona	0.06036	a000793.sp92
S	925	Alphonsina	0.21026	a000925.sp102
S	1036	Ganymed	0.20863	a001036.sp290n1.txt
S	1065	Amundsenia	0.28105	a001065.sp37
S	1131	Porzia	0.24576	a001131.sp28
S	1565	Lemaître	0.08526	a001565.sp36
S	1620	Geographos	0.1875	a001620.sp212.txt
S	1640	Nemo	0.20152	a001640.sp37
S	1660	Wood	0.23431	a001660.sp37
S	1685	Toro	0.107799	a001685.sp266.txt
S	2335	James	0.28533	a002335.sp46
S	6047	1991 TB_1	0.17093	a006047.sp45
S	6386	Keithnoll	0.28876	a006386.sp36
S	6585	O'Keefe	0.15382	a006585.sp55
S	20790	2000 SE_{45}	0.08636	a020790.sp03
S	22771	1999 CU_3	0.30409	a022771.sp26
Sw	32	Pomona	0.23768	a000032.sp76
Sw	63	Ausonia	0.29338	a000063.sp25
Sw	108	Hecuba	0.29611	a000108.sp92
Sw	151	Abundantia	0.47959	a000151.sp47
Sw	192	Nausikaa	0.38015	a000192.sp50

Sw	244	Sita	0.34587	a000244.sp70
Sw	433	Eros	0.37964	a000433.sp245n2.txt
Sw	1139	Atami	0.31543	a001139.sp29
Sw	1204	Renzia	0.33486	a001204.sp37
Sw	1866	Sisyphus	0.39781	a001866.sp56
Sw	1916	Boreas	0.4274	a001916.sp07
Sw	1943	Anteros	0.33296	a001943.sp09
Sw	1980	Tezcatlipoca	0.46433	a001980.sp55
Sw	2074	Shoemaker	0.52025	a002074.sp25
Sw	2107	Ilmari	0.29128	a002107.sp49
Sw	3873	Roddy	0.14955	a003873.sp32
Sw	24475	2000 VN_2	0.31447	a024475.sp105
Sw	98943	2001 CC_{21}	0.45743	au2001CC21.sp33
Sa	984	Gretia	0.4045	a000984.sp92
Sa	5261	Eureka	0.44726	a005261.sp41
Sq	3	Juno	0.26017	a000003.sp96
Sq	11	Parthenope	0.22408	a000011.sp47
Sq	43	Ariadne	0.22921	sp [058]
Sq	720	Bohlinia	0.11762	a000720.sp97
Sq	1374	Isora	0.15982	a001374.sp28
Sq	2063	Bacchus	0.0749	a002063.sp41
Sq	4179	Toutatis	0.15312	a004179.sp228.txt
Sq	4197	1982 TA	0.09432	a004197.sp25
Sq	19356	1997 GH_3	0.13144	a019356.sp03
Sq	35107	1991 VH	0.25816	a035107.sp20
Sq	86819	2000 GK_{137}	0.18331	au2000GK137.sp02
Sqw	39	Laetitia	0.27303	a000039.sp92
Sqw	512	Taurinensis	0.3281	a000512.sp32
Sqw	1494	Savo	0.38019	a001494.sp55
Sqw	2064	Thomsen	0.28628	a002064.sp52
Sqw	3102	Krok	0.27678	a003102.sp02
Sqw	3122	Florence	0.39737	a003122.sp27
Sr	180	Garumna	0.11096	a000180.sp92
Sr	237	Coelestina	0.22916	a000237.sp95
Sr	808	Merxia	0.14752	a000808.sp92
Sr	4558	Janesick	0.15523	a004558.sp29
Sr	5379	Abehiroshi	0.23294	a005379.sp51
Sr	5587	1990 SB	0.06686	a005587.sp224.txt

Sr	5817	Robertfrazer	0.19789	a005817.sp31
Sr	99907	1989 VA	0.20565	au1989VA.sp19
Sr	137062	1998 WM	0.18233	au1998WM.sp19
Srw	3858	Dorchester	0.27082	a003858.sp28
Srw	53435	1999 VM_{40}	0.41676	a053435.sp274n1.txt
V	4	Vesta	0.06325	a000004.sp86
V	3908	Nyx	-0.01697	a003908.sp30
X	22	Kalliope	0.31664	a000022.sp55
X	87	Sylvia	0.29701	a000087.sp44
X	153	Hilda	0.25689	a000153.sp40.txt
Xc	21	Lutetia	0.09331	a000021.sp31
Xe	77	Frigga	0.20909	a000077.sp55
Xe	132	Aethra	0.1142	a000132.sp44
Xe	3103	Eger	0.26716	a003103.sp289.txt
Xk	16	Psyche	0.26212	a000016.sp58
Xk	55	Pandora	0.27962	a000055.sp49
Xk	56	Melete	0.17079	a000056.sp31
Xk	65	Cybele	0.17483	a000065.sp25
Xk	69	Hesperia	0.26176	a000069.sp111
Xk	99	Dike	0.1213	a000099.sp47
Xk	110	Lydia	0.28787	a000110.sp64.txt
Xk	160	Una	0.15767	a000160.sp99
Xk	181	Eucharis	0.05281	a000181.sp25
Xk	201	Penelope	0.21451	a000201.sp28
Xk	250	Bettina	0.28599	a000250.sp26

Note: The spectral types of NEAs and MBAs were cited from Binzel et al. (2019)[7] and DeMeo et al. (2009)[8], respectively. All of the spectral files are collected from the Planetary Spectroscopy at MIT web (http://smass.mit.edu/catalog.php).

Reference

1. Binzel, R. P., Rivkin, A. S., Bus, S. J., Sunshine, J. M. & Burbine, T. H. MUSES-C target asteroid (25143) 1998 SF36: A reddened ordinary chondrite. *Meteorit. Planet. Sci.* **36**, 1167–1172 (2001).
2. Vernazza, P., Binzel, R. P., Rossi, A., Fulchignoni, M. & Birlan, M. Solar wind as the origin of rapid reddening of asteroid surfaces. *Nature* **458**, 993–995 (2009).

3. Dunn, T. L., McCoy, T. J., Sunshine, J. M. & McSween, H. Y. A coordinated spectral, mineralogical, and compositional study of ordinary chondrites. *Icarus* **208**, 789–797 (2010).

4. Cloutis, E. A. *et al.* Spectral reflectance properties of ureilites. *Meteorit. Planet. Sci.* **45**, 1668–1694 (2010).

5. Lucas, M. P., Emery, J. P., Hiroi, T. & McSween, H. Y. Spectral properties and mineral compositions of acapulcoite–lodranite clan meteorites: Establishing S-type asteroid–meteorite connections. *Meteorit. Planet. Sci.* **54**, 157–180 (2019).

6. Moskovitz, N. A., Willman, M., Burbine, T. H., Binzel, R. P. & Bus, S. J. A spectroscopic comparison of HED meteorites and V-type asteroids in the inner Main Belt. *Icarus* **208**, 773–788 (2010).

7. Binzel, R. P. *et al.* Compositional distributions and evolutionary processes for the near-Earth object population: Results from the MIT-Hawaii Near-Earth Object Spectroscopic Survey (MITHNEOS). *Icarus* **324**, 41–76 (2019).

8. DeMeo, F. E., Binzel, R. P., Slivan, S. M. & Bus, S. J. An extension of the Bus asteroid taxonomy into the near-infrared. *Icarus* **202**, 160–180 (2009).